

Classification of Knee Osteoarthritis using CNN

*Umesh Hengaju**

Information and Language Processing Research Lab, Department of Computer Science and Engineering, Kathmandu University, Dhulikhel, Kavre, Nepal

**Corresponding Author*

E-mail Id:-hengajumesh@gmail.com

ABSTRACT

Knee osteoarthritis (OA) is a joint disease which is globally common in elder people. It is typically the result of wear and tear and progressive loss of articular cartilage. It has no cure. Despite of its high prevalence, there is a lack of diagnostic tools and approaches that detects and classifies the different stages of Knee OA severalties with better precision. This paper presents the approaches to automatically quantify the severity of knee OA using X-ray images. Two of the CNN classifiers namely, VGG-15 and ResNet-32 have been used for classifying the knee OA severity into one of the 5 Kellgren-Lawrence classification grades (normal, doubtful, mild, moderate and severe). These models have been trained using loss function: 'categorical cross entropy' and optimizer 'Adam'. The datasets used in this work has been collected from Bhaktapur Hospital. About 350 X-ray images were collected and manually classified into their KL grades and then they were used for testing as well as training the models. The test results shows that the accuracy of classifying knee OA severities with VGG-16 and ResNet-32 were 59% and 57% respectively. It seemed that the accuracy of VGG-16 model is better than ResNet-32 in quantifying knee OA severity.

Keywords:- *Knee osteoarthritis (OA), CNN, VGG-16, ResNet-32, X-ray images, Kellgren-Lawrence classification grades*

INTRODUCTION

Knee Osteoarthritis (OA), also called degenerative joint disease, is a common joint disorder disease in older and overweighed people. It is a highly prevalent chronic joint disease that makes sitting and walking much painful [15]. It is caused due to disintegration of Cartilage. Cartilage is a robust and viscoelastic

connective tissue at the ends of bones which helps in easy movements of bones and abides as a shock absorber. As the Cartilage becomes thin, the gap between bones gets narrow due to which the bones in rubs each other. Thus, there causes severe pain in the joint and it restricts the mobility of bones [12]. According to [3],



Fig.1:-Radiological Image with and without Osteoarthritis.

about 80% of the populations in the world aging 60 years or above have radiographic evidence of Osteoarthritis. And it is expected that Osteoarthritis will become more prevalent in the near future.

Clinically, Knee OA is diagnosed by symptoms and physical examinations. To detect abnormalities in bones and deformed parts of bones, radiographic imaging tools such as X-ray, MRI (Magnetic Resonance Imaging), CT (Computed Tomography) etc. are used [8].

The radiological parameters considered during diagnosis of Knee OA are cartilage disintegration, bones deformation, narrow joint space, osteophytes formation and loose bones [12]. On the basis of radiological parameters and severity levels, a particular joint is assigned to one of the five grades that are given by Kellgren and Lawrence (KL) grading system [1]. Figure 3 shows the different grades of OA disease provided by KL grading system.

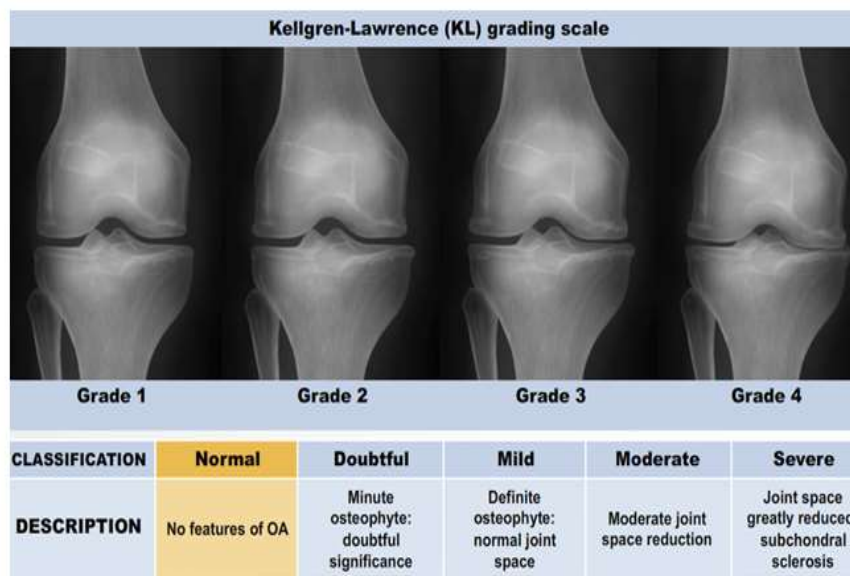


Fig.2:-Kellgren and Lawrence (KL) grading scale

In general, the medical experts manually analyses the radiological images for diagnosing of Knee OA diseases. It is a time consuming work and sometimes the complexities in radiological images makes it difficult to predict the disease efficiently [12]. Emerging trends of technology like computer vision, image processing and pattern recognition is playing an important role in solving such problems.

Various automatic tools and methods have been introduced for detecting and diagnosing the diseases in the field of medical. These tools and methods are, however, extremely, inaccurate and

sensitive [10]. Thus, this paper presents comparative study of the methods for automatically identifying the characteristics of Osteoarthritis. In this work, an automated system is developed using CNN models for detecting severalties of Osteoarthritis in the inputted X-ray images. Two CNN's models, namely, VGG-16 and ResNet-32 are used for developing the system. The system is trained using loss function: 'categorical cross entropy' and optimizer 'Adam'. For training and testing the system, X-ray images collected from Bhaktapur Hospital were used.

The system has been trained and tested with 350 images. The result of test experiment shows that VGG-16 model can quantify knee OA severity with better accuracy as compared to ResNet-32 model.

The rest of the paper comprises related works, problem statement, objectives, proposed methodology, experimental results and conclusion to this work.

RELATED WORKS

In [4], Lior Shamir et al., has described a method for automatic detection of Knee OA. It was based on Kellgren-Lawrence (KL) grading system. In this work, the X-ray images are analyzed and accordingly the knee OA severalties are categorized into five KL grades (normal, doubtful, minimal and moderate).

A simple weighted nearest neighbor rule was used to predict the severalty level of Osteoarthritis. Their model has been experimented with 350 X-ray images and the result of their test experiment shows that moderate OA was differentiated with accuracy of 95% and minimal OA was differentiated with accuracy of 80% from normal OA.

In [8], a method to detect Knee OA using X-ray images has been proposed. It involves predicting the Knee OA by calculating the thickness of cartilage between the bones. Since, the approach involves automated computed measurements; it can be used for better diagnosis of Knee OA.

It was a data driven approach tested with different datasets for diagnosing the osteoarthritis. But this approach only considers the gap between the boned for identifying the characteristics of Osteoarthritis.

In [10], new biomarks for early detection of knee OA in overweight and obese women were identified with the use of Ranked Guided Iterative Feature Elimination (RGIFE) along with random forest algorithm. In the work, a machine learning based pipeline was created to identify small models that predicts 30-month incidence of Knee OA. The result of the work was that the models exhibit performance of $AUC > 0.7$. But, in the work, very few variables were used with the models for quantifying the characteristics of Knee OA.

In [11], Joseph et al., has proposed a method for automatically quantifying the severalties of Osteoarthritis in Knee using X-ray images. It involves using fully convolutional neural network (FCN) for detecting the knee joints and convolutional neural network (CNN) for classifying the severalty level of Knee OA. The model used in this work was evaluated with two public datasets, namely Osteoarthritis Initiative (OAI) and Multicenter Osteoarthritis Study (MOST). The result of the model in detecting and classifying the knee OA severity was quite promising.

In [12], Shivanand et al., used Artificial Neural Network (ANN) for analyzing the knee radiographic images and quantifying the severalty of Knee OA into five KL grades. In their work, about 1650 radiological images were collected from different hospitals and those images were annotated into KL grade by two different surgeons as per KL grading system. Then, the local phase quantization and multi-block projection profile features are computed and fed into artificial neural network classifier for automating the KL grading procedure. The classifying accuracy of this work in classifying the knee X-ray images into KL grading of the OA severalty was 98.7% and 98.2%

respectively with reference to opinions of Surgeon-1 and surgeon-2.

In [13], Mahrukh et al., has presented a system that automatically detects the knee OA from X-ray images. In the system template matching technique was used for detecting tibiofemoral joint regions. In this work, the joint space width is calculated by detecting the boundaries of ROI in the histogram orientation and based on this information; severity of Knee OA is quantified. This work exhibit an accuracy of 97.14% in quantifying the severalties of Knee OA. In this work, the region of interest (ROI) is cropped automatically and the whole process is semi-automatic and the required image can be clean or noisy without manual assistance.

PROBLEM STATEMENT

Traditional approach of diagnosis by doctors has always been time consuming and sometimes become inaccurate to some extent. This may lead to false diagnosis, affecting patient’s health in a very minor or major way. Minor effects can be negligible but major effects may be life threatening [12]. Thus, there has always been a need of tools and techniques for correct diagnosis of diseases. And,

emerging technology like computer vision, image processing and pattern recognition have overcome the limitations with better prediction of diseases, diagnosis and treatments [10]. Many powerful tools such as image machine learning, deep learning, neural network etc. are being widely used in the medical filed for bringing qualitative information and diagnosing the diseases with better accuracy. But, the available tools and techniques for diagnosing the diseases are not accurate and are low sensitive.

OBJECTIVES

The objective of this work is as follows:

1. To identify the differences in the joints between normal and abnormal knees using X-ray images.
2. To quantify the severalties of knee OA in the abnormal knee via use of convolutional neural network (CNN) models.

METHODOLOGY

Figure 3 shows the overall framework for the given work. The work here comprises of five main steps: Preprocessing, Image segmentation, Image Enhancement, Feature Extraction and Classification.

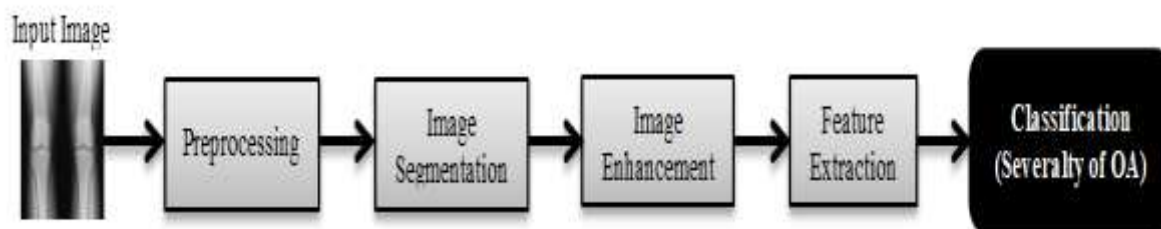


Fig.3:-Block Diagram of the proposed framework

Preprocessing

The X-ray images of knee are preprocessed with an aim to improve the quality of the image so that bone edges can be easily detected and severity of Osteoarthritis can be easily quantified [12]. The radiological images of knee may

contain salt and pepper noise. To remove such noise from the image by preserving bone edges of the knee, adaptive median filter have been used. Also, the Knee X-ray images are resized to 256*256 after cropping the image for proper analysis.



Fig.4:-Original Image



Fig.5:-Preprocessed Image

Image Segmentation

Segmentation of knee X-ray images are done to partition the object into its constituent parts so that the features can be easily extracted and the object can be recognized [2]. In this work, active

contour segmentation method has been used for segmentation of X-ray image. During segmentation process, the region in between tibia and femur are segmented and are processed for further processing.

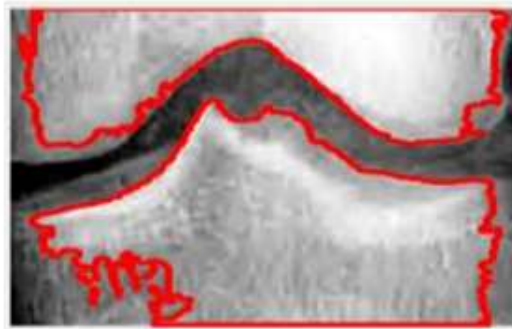


Fig.6:-Segmented Image

Image Enhancement

Image Enhancement is done to improve the perception of information or interpretability in the image. It involves improving the quality (clarity) of image in terms of contrast, shading unsharp

masking etc. [5] In this work, the radiological image of knee has been enhance via adjusting contrast. For the purpose, histogram equalization method has been implemented.



Fig.7:-Enhanced Image

Feature Extraction

It involves extracting the useful information from machine readable document in order to minimize the intra-class pattern variability and maximize the inter-class pattern variability of the content in the document [6]. The various features extracted in this work are Statistical Features, Shape Features and Haralick Features.

$$\text{Mean } (\mu) = \sum_{i,j} p(i, j)$$

$$\text{Median} = \sum_{i,j} \{p(i, j)\} / \{(i, j)\}$$

$$\text{Standard Deviation} = \sqrt{\frac{1}{N-1} \sum_{i=1}^N |A_i - \mu|^2}$$

$$\text{Variance } (\sigma) = \frac{1}{N-1} \sum_{i=1}^N |A_i - \mu|^2$$

$$\text{Skewness} = \frac{E(x-\mu)^2}{\sigma^3}$$

$$\text{Kurtosis} = \frac{E(x-\mu)^4}{\sigma^4}$$

Shape feature extraction

These features refer to measuring the similarities of the shapes. Shape features are calculated from connected components that are stored in contiguous and dis-contiguous regions [6].

Area (A) = number of pixels of an image

Perimeter (P) = number of boundary pixels

$$\text{Eccentricity (E)} = \frac{\lambda_1}{\lambda_2}$$

$$\text{Equiv-diameter} = \sqrt{(4 * \frac{Area}{\pi})}$$

Euler Number = (number of objects) – (number of holes)

$$\text{Solidity (S)} = \frac{\text{Area}}{\text{convex area}}$$

Major Axis Length = length of major axis of an object in pixels.

Minor Axis Length = length of minor axis of an object in pixels.

Haralick feature extraction:

These features refer to measuring the texture of the knee image in terms of contrast, correlation, sum of squares, sum

Statistical feature extraction

Statistical features are quantitative measurements of relationships between various sets of points [12]. In this work, various statistical measures like mean, median, standard deviations, variance, kurtosis and Skewness were used. Equations representing these statistical features are as follows. Each of the statistical properties is calculated based on the pixels p (i, j) themselves.

The various shape features considered in this work are area, perimeter, eccentricity, equiv-diameter, Euler Number, solidity, major axis length and minor axis length.

of average, homogeneity etc. [12] The various Haralick features considered in this work are contrast, correlation, energy and homogeneity.

$$\text{Contrast} = \sum_{i,j} |i - j|^2 p(i, j)$$

$$\text{Correlation} = \sum_{i,j} \frac{(i-\mu_i)(j-\mu_j) p(i, j)}{\sigma_i \sigma_j}$$

$$\text{Energy} = \sum_{i,j} p(i, j)^2$$

$$\text{Homogeneity} = \sum_{i,j} \frac{p(i, j)}{1+|i-j|}$$

| FEATURE EXTRACTION | |
|--------------------|----------|
| Skewness | -0.3833 |
| Kurtosis | 1.1469 |
| Variance | 0.054312 |
| Standard deviation | 0.49107 |
| Mean | 0.59411 |
| Entropy | 0.97429 |
| Contrast | 0.010731 |
| Correlation | 0.97771 |
| Energy | 0.50801 |
| Homogeneity | 0.99463 |
| Area | 100 |
| Eccentricity | 0 |
| Euler Number | 1 |
| Equiv diameter | 1.1284 |
| Perimeter | 0 |
| Major axis length | 1.1547 |
| Minor axis length | 1.1547 |

Fig.8:-Feature Extracted Image

Classification

After the features have been extracted, some classification methods are employed for classification of knee OA severity into five KL grades. Two different type of classifier models have been used for quantifying the severalties of Knee OA, namely, VGG-16 and ResNet-32.

VGG-16

VGG-16 (also called OxfordNet) is a convolutional neural network architecture named after the Visual Geometry Group from Oxford, who developed it. It was proposed by K. Simonyan and A. Zisserman from the University of Oxford in the paper “Very Deep Convolutional

Networks for Large-Scale Image Recognition” [17]. It was one of the famous model submitted to ILSVRC-2014 while achieving 1st runner-up position with the winner being GoogLeNet. This is an improvement over AlexNet by replacing large kernel-sized filters (11 and 5 in the first and second layers, respectively) with multiple 3*3 kernel-sized filters in succession. A test data set with over 14 million images was used to validate the model, which achieved 92.7% accuracy [16].

Architecture of VGG-16

The architecture of VGG-16 can be depicted as:



Fig.9:-VGG-16 Architectural Map

The input to conv1 layer is of fixed size 224 x 224 RGB image. The image is passed through a stack of convolutional (conv.) layers, where the filters were used with a very small receptive field: 3x3 (which is the smallest size to capture the notion of left/right, up/down, center).

In one of the configurations, it also utilizes 1x1 convolution filters, which can be seen as a linear transformation of the input channels (followed by non-linearity). The convolution stride is fixed to 1 pixel; the spatial padding of conv. layer input is such that the spatial resolution is preserved after convolution, i.e. the padding is 1-pixel for 3x3 conv. layers. Spatial pooling is carried

out by five max-pooling layers, which follow some of the convolution layers (not all the conv. layers are followed by max-pooling). Max-pooling is performed over a 2x2 pixel window, with stride 2 [18].

Three fully connected (FC) layers follow a stack of convolution layers (which has a different depth in different architectures): the first two have 4096 channels each, the third performs 1000-way ILSVRC classification and thus contains 1000 channels (one for each class). The final layer is a soft-max layer. The configuration of the fully connected layers is the same in all networks [18].

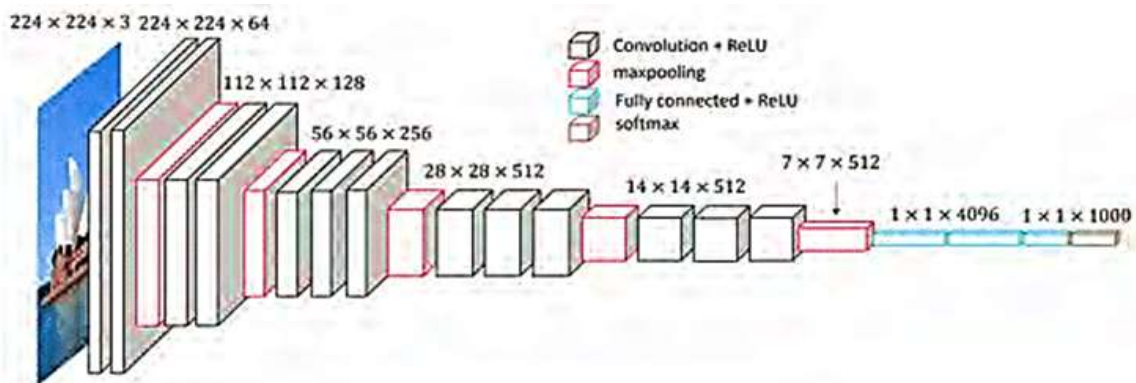


Fig.10:-VGC-16Architecture

Configuration for VGG-16

All configurations follow the generic design present in architecture and differ only in the depth: from 11 weight layers in the network ‘A’ (8 conv. and 3 FC layers) to 19 weight layers in the network E (16

conv. and 3 FC layers). The width of conv. layers (the number of channels) is rather small, starting from 64 in the first layer and then increasing by a factor of 2 after each max-pooling layer, until it reaches 512 [18].

| ConvNet Configuration | | | | | |
|-----------------------------|------------------------|-------------------------------|--|--|---|
| A | A-LRN | B | C | D | E |
| 11 weight layers | 11 weight layers | 13 weight layers | 16 weight layers | 16 weight layers | 19 weight layers |
| input (224 × 224 RGB image) | | | | | |
| conv3-64 | conv3-64 LRN | conv3-64 conv3-64 | conv3-64 conv3-64 | conv3-64 conv3-64 | conv3-64 conv3-64 |
| maxpool | | | | | |
| conv3-128 | conv3-128 | conv3-128 conv3-128 | conv3-128 conv3-128 | conv3-128 conv3-128 | conv3-128 conv3-128 |
| maxpool | | | | | |
| conv3-256 conv3-256 | conv3-256 conv3-256 | conv3-256 conv3-256 | conv3-256 conv3-256 conv1-256 | conv3-256 conv3-256 conv3-256 | conv3-256 conv3-256 conv3-256 conv3-256 |
| maxpool | | | | | |
| conv3-512 conv3-512 | conv3-512 conv3-512 | conv3-512 conv3-512 | conv3-512 conv3-512 conv1-512 | conv3-512 conv3-512 conv3-512 | conv3-512 conv3-512 conv3-512 conv3-512 |
| maxpool | | | | | |
| conv3-512 conv3-512 | conv3-512 conv3-512 | conv3-512 conv3-512 | conv3-512 conv3-512 conv1-512 | conv3-512 conv3-512 conv3-512 | conv3-512 conv3-512 conv3-512 conv3-512 |
| maxpool | | | | | |
| FC-4096 | | | | | |
| FC-4096 | | | | | |
| FC-1000 | | | | | |
| soft-max | | | | | |

Fig.11:-Architectural Configuration for VGG-16

ResNet-32

A residual neural network (ResNet) is an artificial neural network (ANN) of a kind that builds on constructs known from pyramidal cells in the cerebral cortex. ResNet-32 is a convolutional neural network backbone derived from ResNet-34, ResNet-50, and ResNet-101 networks [9]. It has an issue of vanishing/exploding gradient.

In order to solve this issue, concept of Residual Network is introduced in the architecture of ResNet [7]. For the purpose, a technique called skip connection and identity mapping is used.

The skip connection skips training from a few layers and connects directly to the output. This identity mapping does not have any parameters and is just there to add the output from the previous layer to the layer ahead [14].

Architecture of ResNet-32

The architecture of ResNet-32 is mostly inspired by ResNet-34's architecture. Figure given below illustrates the architecture of ResNet-32. In the ResNet-32's architecture, shortcut connections are added which are then converted into residual network [9].

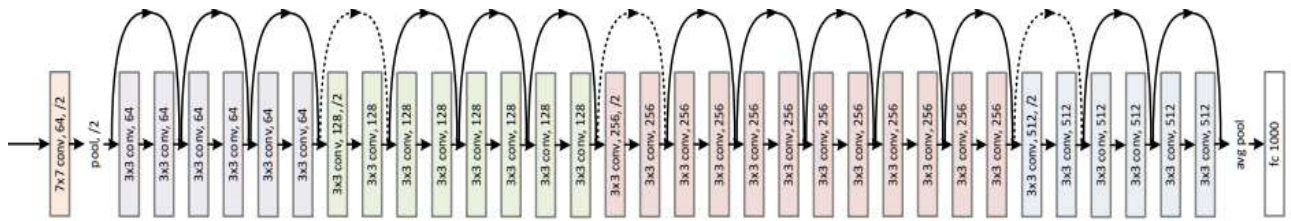


Fig.12:-ResNet-32 Architecture

Configuration for ResNet-32

Each ResNet-32 block is either two layers deep (used in small networks like ResNet

18, 34) or 3 layers deep (ResNet 50, 101, 152). The configurations of ResNet-32 based on its architecture can be overall represented as given below [9]:

| layer name | output size | 18-layer | 34-layer | 50-layer | 101-layer | 152-layer |
|------------|-------------|---|---|---|--|--|
| conv1 | 112x112 | 7x7, 64, stride 2 | | | | |
| conv2_x | 56x56 | 3x3 max pool, stride 2 | | | | |
| | | $\begin{bmatrix} 3 \times 3, 64 \\ 3 \times 3, 64 \end{bmatrix} \times 2$ | $\begin{bmatrix} 3 \times 3, 64 \\ 3 \times 3, 64 \end{bmatrix} \times 3$ | $\begin{bmatrix} 1 \times 1, 64 \\ 3 \times 3, 64 \\ 1 \times 1, 256 \end{bmatrix} \times 3$ | $\begin{bmatrix} 1 \times 1, 64 \\ 3 \times 3, 64 \\ 1 \times 1, 256 \end{bmatrix} \times 3$ | $\begin{bmatrix} 1 \times 1, 64 \\ 3 \times 3, 64 \\ 1 \times 1, 256 \end{bmatrix} \times 3$ |
| conv3_x | 28x28 | $\begin{bmatrix} 3 \times 3, 128 \\ 3 \times 3, 128 \end{bmatrix} \times 2$ | $\begin{bmatrix} 3 \times 3, 128 \\ 3 \times 3, 128 \end{bmatrix} \times 4$ | $\begin{bmatrix} 1 \times 1, 128 \\ 3 \times 3, 128 \\ 1 \times 1, 512 \end{bmatrix} \times 4$ | $\begin{bmatrix} 1 \times 1, 128 \\ 3 \times 3, 128 \\ 1 \times 1, 512 \end{bmatrix} \times 4$ | $\begin{bmatrix} 1 \times 1, 128 \\ 3 \times 3, 128 \\ 1 \times 1, 512 \end{bmatrix} \times 8$ |
| conv4_x | 14x14 | $\begin{bmatrix} 3 \times 3, 256 \\ 3 \times 3, 256 \end{bmatrix} \times 2$ | $\begin{bmatrix} 3 \times 3, 256 \\ 3 \times 3, 256 \end{bmatrix} \times 6$ | $\begin{bmatrix} 1 \times 1, 256 \\ 3 \times 3, 256 \\ 1 \times 1, 1024 \end{bmatrix} \times 6$ | $\begin{bmatrix} 1 \times 1, 256 \\ 3 \times 3, 256 \\ 1 \times 1, 1024 \end{bmatrix} \times 23$ | $\begin{bmatrix} 1 \times 1, 256 \\ 3 \times 3, 256 \\ 1 \times 1, 1024 \end{bmatrix} \times 36$ |
| conv5_x | 7x7 | $\begin{bmatrix} 3 \times 3, 512 \\ 3 \times 3, 512 \end{bmatrix} \times 2$ | $\begin{bmatrix} 3 \times 3, 512 \\ 3 \times 3, 512 \end{bmatrix} \times 3$ | $\begin{bmatrix} 1 \times 1, 512 \\ 3 \times 3, 512 \\ 1 \times 1, 2048 \end{bmatrix} \times 3$ | $\begin{bmatrix} 1 \times 1, 512 \\ 3 \times 3, 512 \\ 1 \times 1, 2048 \end{bmatrix} \times 3$ | $\begin{bmatrix} 1 \times 1, 512 \\ 3 \times 3, 512 \\ 1 \times 1, 2048 \end{bmatrix} \times 3$ |
| | 1x1 | average pool, 1000-d fc, softmax | | | | |
| FLOPs | | 1.8×10^9 | 3.6×10^9 | 3.8×10^9 | 7.6×10^9 | 11.3×10^9 |

Fig.13:-Architectural Configuration for ResNet-32

Experimentation

A system was developed based on the proposed framework for performing test experiment. The system was developed with two of the CNN classifier model, namely, VGG-16 and ResNet-32. The system with both of the classifier models was first trained and then tested with the

generated dataset separately. During training process of the model, a feature database was created in which the trained information were stored. This information was used for quantifying the severalty of knee OA in testing process. Figure 14 depicts an overview of the developed system.

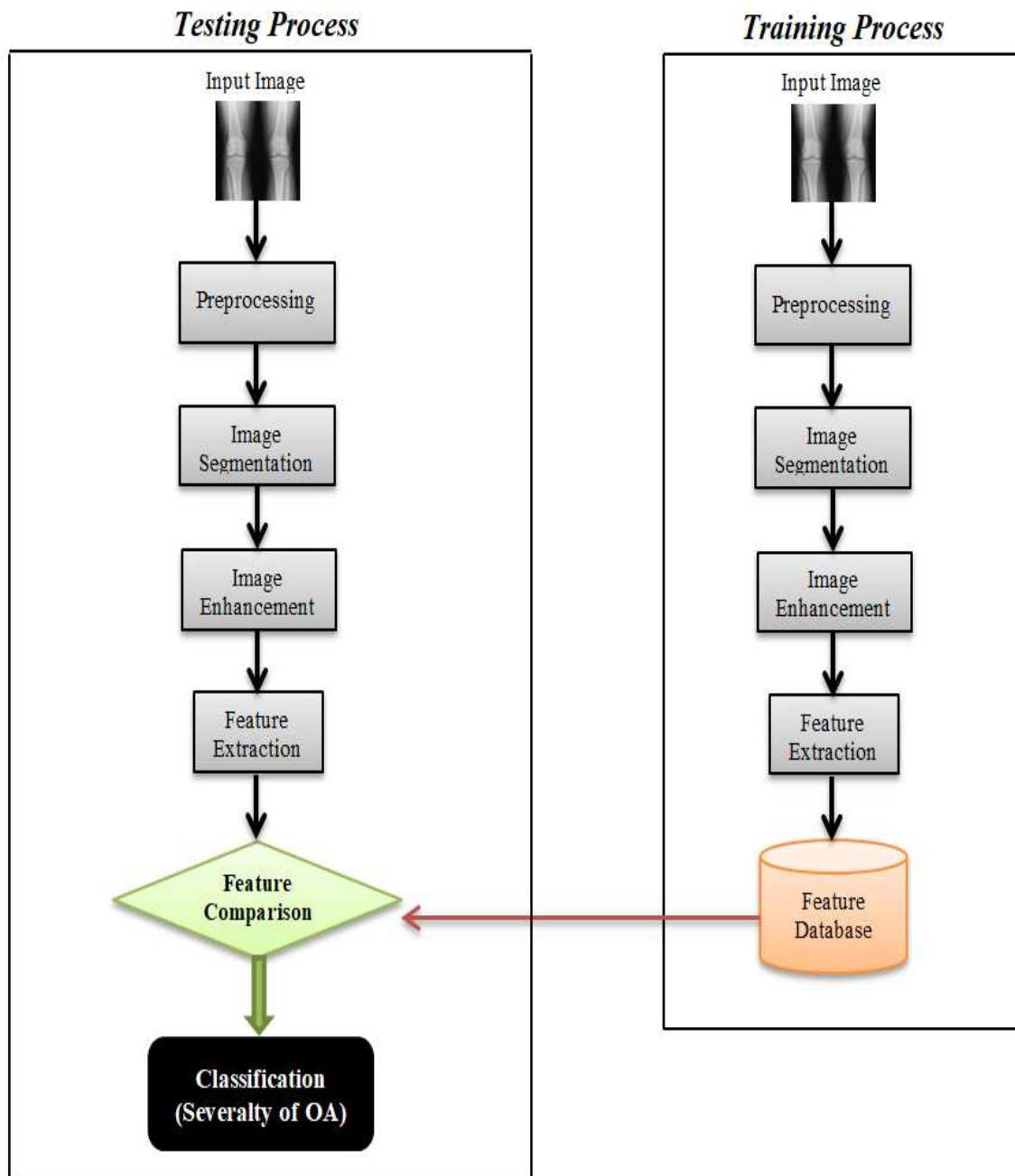


Fig.14:- Overview of the developed system

Dataset

The data used in the experimentation process of the developed system are the knee X-ray images. Thus, X-ray images of knee were collected from Bhaktapur Hospital.

Around 350 knee X-ray images were collected. Among the collected knee X-ray images, 60% of the images were used in

training the model and 40% of the images were used for testing the model.

RESULT AND DISCUSSION

The system successfully classified the X-ray images into their constituent classes with desired level of accuracy. The result of the test experiment with the developed system is shown in the figure below:

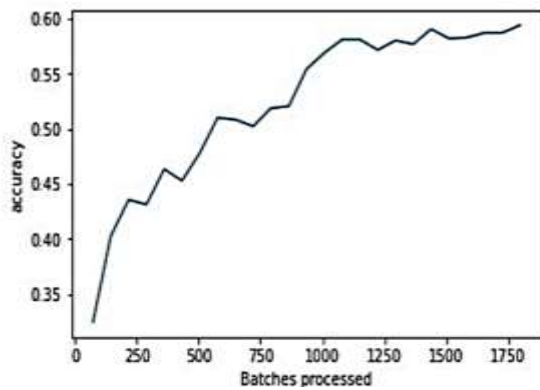


Fig.15:-Accuracy with VGG-16

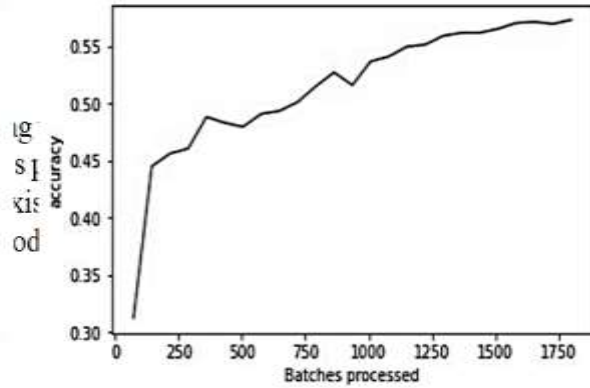


Fig.16:-Accuracy with ResNet-32

Figure 15 and Figure 16 show a graph exhibiting the accuracy with the two models. In these graph, the X-axis denotes the number of batches processed i.e. it shows that a single epoch consists of

processing of 250 batches. And Y-axis denotes the accuracy obtained in each batch. The accuracy with VGG-16 classifier model is 59% and with ResNet-32 classifier model is 57%.

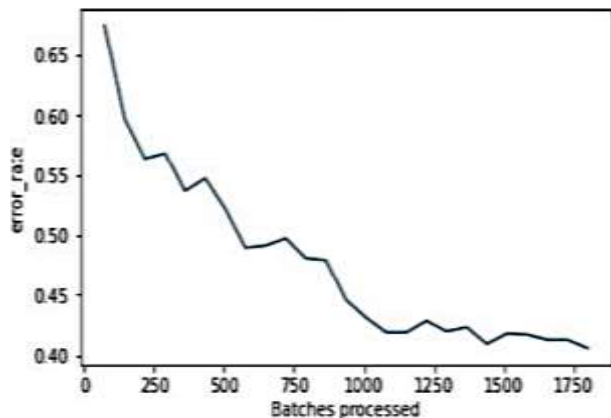


Fig.17:-Error rate with VGG-16

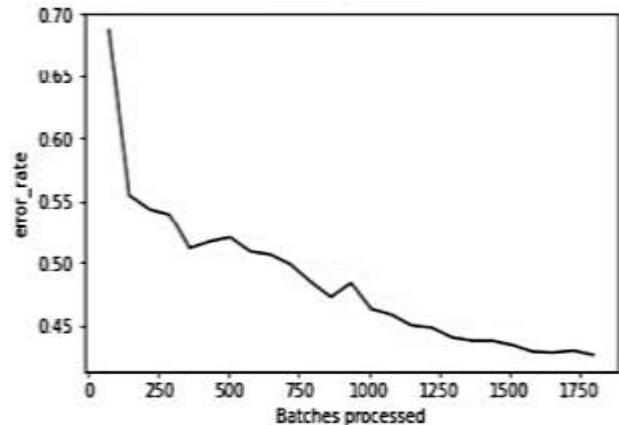


Fig.18:-Error rate with ResNet-32

Figure 17 and Figure 18 shows a graphs presenting error rate with the two classifier models. These graphs depicts that with the increase in number of epoch consisting of 250 batches the error rate gets decreased. However, the error rate of classifier with VGG-16 40% and with ResNet-32 is 41%.

and ResNet-32 for quantifying the severalties of Knee OA into five KL grades. The main aim of this work was to compare the accuracy in classifying the severalties of Osteoarthritis with the two models i.e. VGG-16 and ResNet-32.

CONCLUSION

This paper presents approaches for detecting Knee OA and classifying the severalties of Osteoarthritis using X-ray images. In the given work, two of the CNN classifier models, namely, VGG-16

For the purpose, a system was developed with both VGG-16 and ResNet-32 classifier and it was experimented with the X-ray images of knee.

The result of test experiment shows that VGG-16 classifier provides better

accuracy in quantifying severalties of Knee OA as compared to ResNet-32.

REFERENCES

1. Kellgren, J. H., & Lawrence, J. (1957). Radiological assessment of osteo-arthrosis. *Annals of the rheumatic diseases*, 16(4), 494.
2. Behiels, G., Vandermeulen, D., Maes, F., Suetens, P., & Dewaele, P. (1999, September). Active shape model-based segmentation of digital X-ray images. In *International Conference on Medical Image Computing and Computer-Assisted Intervention* (pp. 128-137). Springer, Berlin, Heidelberg.
3. St Clair SF, Higuera C, Krebs V, Tadross NA, Dumpe J, Barsoum (2006). Hip and Knee Arthroplasty in the Geriatric Population. *Clin Geriatr Med* 2006;3:515–533. [PubMed: 16860243]
4. Shamir, L., Ling, S. M., Scott, W. W., Bos, A., Orlov, N., Macura, T. J., ... & Goldberg, I. G. (2008). Knee x-ray image analysis method for automated detection of osteoarthritis. *IEEE Transactions on Biomedical Engineering*, 56(2), 407-415..
5. Bandyopadhyay, S. K. (2011). An edge detection algorithm for human knee osteoarthritis images. *Journal of Global Research in Computer Science*, 2(4).
6. Deokar, D. D., & Patil, C. G. (2015). Effective feature extraction based automatic knee osteoarthritis detection and classification using neural network. *International Journal of Engineering and Techniques*, ISSN, 2395-1303.
7. He, K., Zhang, X., Ren, S., & Sun, J. (2016). Deep residual learning for image recognition. In *Proceedings of the IEEE conference on computer vision and pattern recognition* (pp. 770-778).
8. Targ, S., Almeida, D., & Lyman, K. (2016). Resnet in resnet: Generalizing residual architectures. *arXiv preprint arXiv:1603.08029*.
9. Lazzarini, N., Runhaar, J., Bay-Jensen, A. C., Thudium, C. S., Bierma-Zeinstra, S. M. A., Henrotin, Y., & Bacardit, J. (2017). A machine learning approach for the identification of new biomarkers for knee osteoarthritis development in overweight and obese women. *Osteoarthritis and cartilage*, 25(12), 2014-2021.
10. Antony, J., McGuinness, K., Moran, K., & O'Connor, N. E. (2017, July). Automatic detection of knee joints and quantification of knee osteoarthritis severity using convolutional neural networks. In *International conference on machine learning and data mining in pattern recognition* (pp. 376-390). Springer, Cham.
11. Gornale, S. S., Patravali, P. U., & Hiremath, P. S. (2019). Detection of osteoarthritis in knee radiographic images using artificial neural network. *Int. J. Innovat. Technol. Explor. Eng*, 8, 2429-2434.
12. Saleem, M., Farid, M. S., Saleem, S., & Khan, M. H. (2020). X-ray image analysis for automated knee osteoarthritis detection. *Signal, Image and Video Processing*, 14(6), 1079-1087.
13. Mujtaba, H. (2020). *Introduction to resnet or residual network*. Technical report, <https://www.mygreatlearning.com/blog/resnet>.
14. Zheng, K., Wang, Y., Hsieh, C. I., Lu, L., Xiao, J., Kuo, C. F., & Miao, S. (2021). Coherence Learning using Keypoint-based Pooling Network for Accurately Assessing Radiographic Knee Osteoarthritis. *arXiv preprint arXiv:2112.09177*.

15. Avinash T., *Introduction to VGG16 / what is VGG16?* Computer Vision (2021).
16. Simonyan, K., & Zisserman, A. (2014). Very deep convolutional networks for large-scale image recognition. *arXiv preprint arXiv:1409.1556*.
17. Chebbi, I. (2021). VGG16: Visual Generation of Relevant Natural Language Questions from Radiology Images for Anomaly Detection.